



HAL
open science

Ozone compatibility with polymer nanofiltration membranes

Sara Ouali, Patrick Louergue, Pierre-Francois Biard, Nouredine Nasrallah,
Anthony Szymczyk

► **To cite this version:**

Sara Ouali, Patrick Louergue, Pierre-Francois Biard, Nouredine Nasrallah, Anthony Szymczyk. Ozone compatibility with polymer nanofiltration membranes. *Journal of Membrane Science*, 2021, 618, pp.118656. 10.1016/j.memsci.2020.118656 . hal-02960372

HAL Id: hal-02960372

<https://hal.science/hal-02960372>

Submitted on 30 Nov 2020

HAL is a multi-disciplinary open access archive for the deposit and dissemination of scientific research documents, whether they are published or not. The documents may come from teaching and research institutions in France or abroad, or from public or private research centers.

L'archive ouverte pluridisciplinaire **HAL**, est destinée au dépôt et à la diffusion de documents scientifiques de niveau recherche, publiés ou non, émanant des établissements d'enseignement et de recherche français ou étrangers, des laboratoires publics ou privés.

Ozone compatibility with polymer nanofiltration membranes

Sara Ouali^{1,2}, Patrick Loulergue¹, Pierre-François Biard¹, Noureddine Nasrallah², Anthony Szymczyk^{1*}

¹*Univ Rennes 1, Ecole Nationale Supérieure de Chimie de Rennes, CNRS, ISCR (Institut des Sciences Chimiques de Rennes) – UMR 6226, F-35000 Rennes, France.*

²*Faculté de Génie Mécanique et Génie des Procédés, Université des Sciences et de la Technologie Houari Boumediene, Algiers, Algeria.*

*Corresponding author: anthony.szymczyk@univ-rennes1.fr

Abstract

Ozone is a strong oxidant applied in water treatment for disinfection and organic and inorganic pollutants removal. It can be coupled with membrane processes as a pre-treatment or post-treatment as well as in a hybrid configuration. In this study, we investigated the resistance of three commercial polymer nanofiltration membranes (NP10, NF90 and NF270) in contact with ozone (10 ppm for 1 h) at pH 3 and 7 to assess the influence of the ozone to hydroxyl radical concentrations balance. The surface properties of membranes were characterized before and after ozonation by means of various techniques, i.e. Fourier transform infrared spectroscopy in attenuated total reflectance mode (ATR-FTIR), zeta potential, water contact angle, X-ray photoelectron spectroscopy (XPS), atomic force microscopy (AFM) and scanning electron microscopy (SEM). For all membranes, the impact of ozonation on pure water permeability was greater at pH 7 than pH 3 due to the faster decomposition of ozone at pH 7 leading to the formation of more free radicals. A decrease in the NP10 membrane permeability (up to 25%) was obtained after ozonation. ATR-FTIR, zeta potential and SEM revealed a fairly good resistance of the polyethersulfone (PES) matrix to ozonation (thanks to the protective effect of electron-withdrawing sulfone groups) under the exposure conditions of this study but the polyvinylpyrrolidone (PVP) additive was substantially oxidized. XPS indicated that the degraded PVP was not released from the PES matrix. It was suggested that the decrease in the NP10 membrane permeability might result from a cross-linking process between macroradicals of degraded PVP chains. In contrast to what was observed with the NP10 membrane, the pure

water permeability of the thin-film composite polyamide (PA) membranes dramatically increased after ozonation. The fully aromatic NF90 membrane appeared to be even more sensitive to ozone than the semi aromatic NF270. The different resistances of NF90 and NF270 membranes were attributed to the different amine monomers used for the synthesis of their active layer. Indeed, m-phenylenediamine used in interfacial polymerization of the NF90 active layer is an aromatic amine (aromatic rings are sensitive to ozonation) and is less basic than the non-aromatic piperazine used to develop the NF270 membrane (protonation of amines contributes to protect them from electrophilic attacks). For both PA membranes, ATR-FTIR and SEM indicated severely damaged active layers. The very sharp increase in the NF90 and NF270 permeabilities was attributed to the removal of active layer fragments, which was found compatible with both zeta potential and water contact angle measurements.

Keywords: Nanofiltration, ozone, polyethersulfone, polyvinylpyrrolidone, polyamide.

1. Introduction

The global demand for membrane processes has been steadily growing due to their numerous advantages in terms of environmental foot print. Pressure-driven membrane processes, which include microfiltration (MF), ultrafiltration (UF), nanofiltration (NF) and reverse osmosis (RO), are widely used for water treatment. Nowadays, one of the major concerns is the presence of toxic pollutants in water streams such as pesticide, endocrine disrupting compounds and pharmaceutical agents. NF is a separation process whose molecular weight cut-off (MWCO) lies in the range $\sim 200 - 1000$ Da [1]. NF membranes can therefore reject a wide range of small organic and inorganic compounds [2,3] and provide high quality water for various applications [4–6].

To date, most NF membranes are thin-film composite (TFC) membranes made of a polyamide (PA) active layer on top of a polysulfone (PSf) microporous support reinforced with a nonwoven substrate [7]. Although the exact composition is not fully disclosed by suppliers, it is well known that most TFC PA membranes are made by interfacial polymerization between trimesoyl chloride (TMC) and *m*-phenylenediamine (MPD) or piperazine (PIP) [8,9]. Some of the low MWCO polyethersulfone (PES) membranes can also support NF applications. The main drawback of PES is its relatively hydrophobic character. Thus, one effective way to produce hydrophilic PES membranes is to incorporate hydrophilic agents such as polyvinylpyrrolidone (PVP), chitosan, polyethylene oxide or polyethylene glycol via additive blending [10].

Membrane fouling is the main drawback of pressure-driven membrane processes. It can be defined as the decrease of filtration performance due to the accumulation of the rejected compounds at the membrane surface and/or inside pores. Organic and inorganic compounds can accumulate on membrane surface and form a cake or gel layer, which may cause a significant increase of the hydraulic resistance, thus leading to the reduction of the membrane permeability and a substantial increase in operating and maintenance costs [11–13]. Although considerable efforts have been made to reduce the occurrence of membrane fouling, chemical treatments are needed on a regular basis to clean the membranes.

An option to mitigate membrane fouling consists in pre-treating the feed solution in order to reduce the amount of foulant species. It can be done by means of ozone (O_3), which has been recognized for its disinfectant and oxidative actions in drinking and wastewater treatments. Ozonation combined with membrane separations offers new opportunities [14]. Indeed, NF is a separation process enabling micropollutants concentration while ozonation is a destructive

technique able to eliminate micropollutants and break down membrane foulants very effectively [4]. O_3 is a strong oxidant that can affect a great variety of organic micropollutants including many pesticides, drugs, etc. [15]. Its reactivity in water is due to both direct reactions with molecular ozone and indirect reactions involving radicals generated during ozone decomposition in water [4,16–18]. O_3 being strongly electrophilic, it reacts easily with double bonds, electron-rich aromatic systems, amines, sulfides, etc... The stability of ozone in water strongly depends on the water matrix [19]. Ozone decomposition in natural water can be initiated thanks to reactions with hydroxide anions, some moieties from natural organic matter and some inorganic compounds (e.g. hydroperoxide anions)[20]. This decomposition leads to radical chain cycles involving several free radicals such as hydroxyl radicals (HO^\bullet) or superoxide radicals ($O_2^{\bullet-}$) [16,20]. Thus, the properties of the water matrix strongly affect ozone decomposition, especially the pH, the organic matter content and the hydrogen carbonate concentration. Typically, an increase in the pH leads to a faster ozone decomposition rate and a higher free radicals generation [19,20]. Hydroxyl radicals are considered as the main reactive species generated during ozone decomposition [21]. They are extremely reactive (most reactions with organic compounds have reaction rate constants in the range 10^7 - 10^9 L mol⁻¹ s⁻¹) and poorly selective [17].

Different studies were dedicated to coupling of ozonation and membrane processes, including ozonation as a pre-treatment or post-treatment step as well as hybridization of both processes or use of membrane contactor to achieve ozone transfer in solution [22–37]. Although inorganic membranes have been recommended for coupling with ozonation (due to their high chemical resistance), polymeric membranes are usually used for water treatment applications because of lower manufacturing cost. Some authors investigated the resistance of polymer materials in contact with ozone. For instance, Goto et al. studied the chemical reactivity of various polymers with ozone and showed the greater sensitivity of polymers containing C=C double bonds compared with polymers having only single C-C bonds [38]. It should be stressed, however, that studies addressing the impact of ozone on polymer membranes are scarce [15,39]. The aim of this work was therefore to assess the resistance of several NF polymer membranes when exposed to dissolved ozone at two different pH in order to assess the influence of the ozone to free radicals balance (3 and 7). The membranes were characterized by various techniques before and after exposure to ozone in order to gain insights into the impact of ozonation on their surface properties. Modifications of the latter were then correlated with variations of the membrane pure water permeability.

2. Material and methods

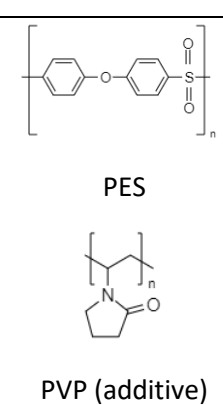
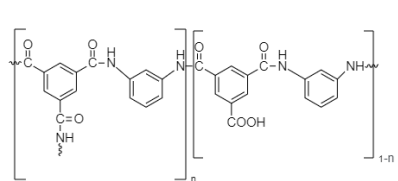
2.1. Chemicals

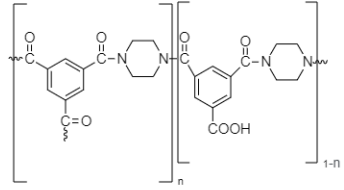
Electrolyte solutions used for electrokinetic measurements were prepared from potassium chloride (KCl) (> 99%, Fisher Scientific) and deionized (DI) water. Potassium hydroxide (KOH), sodium hydroxide (NaOH) and hydrochloric acid (HCl) were used for pH adjustment. Ethanol (>99%, Fischer Scientific) was used to prepare water/ethanol mixtures in order to clean membranes and remove potential preservative agents prior to use. Tertiobutanol (Acros Organics, analytical grade) was used as a free radical scavenger.

2.2 Membranes

Three commercial flat-sheet NF membranes were used in this study: a PES-based membrane (NP10 from Microdyn Nadir) and two TFC PA membranes (NF270 and NF90 from Dow Filmtec) made of different monomers. The chemical structures of these polymer membranes are shown in Table 1.

Table 1. NF membranes used in this work.

Membrane	Manufacturer	Active layer	MWCO (Da)	Chemical structure of the active layer
NP10	Microdyn Nadir	Polyethersulfone (PES) + polyvinylpyrrolidone (PVP)	1000-1200	 <p>The image shows the chemical structures of the active layer components for the NP10 membrane. It includes the structure of Polyethersulfone (PES), which is a repeating unit of a polymer chain consisting of two phenylene rings connected by an oxygen atom and a sulfone group (SO₂). Below it is the structure of Polyvinylpyrrolidone (PVP), which is a five-membered pyrrolidone ring with a vinyl group attached to the nitrogen atom. The structures are labeled 'PES' and 'PVP (additive)' respectively.</p>
NF90	Dow Filmtec	Fully aromatic polyamide (PA)	100 - 200	 <p>The image shows the chemical structure of a fully aromatic polyamide (PA) monomer. It consists of two aromatic rings connected by an amide bond (-NH-CO-). One of the aromatic rings has a carboxylic acid group (-COOH) and a sulfonamide group (-NH-SO₂-NH₂) attached to it. The structure is shown as a repeating unit with a subscript 'n' and a subscript '1-n'.</p>

NF270	Dow Filmtec	Semi aromatic polyamide (PA)	200 - 300	
-------	-------------	------------------------------	--------------	---

2.3. Membrane ozonation set-up and procedure

Before use, all membranes were cleaned to remove potential preservative agents according to the following protocol: sonication in a 50/50 (v/v) water/ethanol mixture followed by rinsing with DI water and sonication (twice for 2 min). After cleaning, all membrane coupons were stored in DI water. The membranes were further exposed to ozonated water according to the following procedure. Two liters of ultra-pure water were set at pH 3 or 7 using hydrochloric acid (1 M) and sodium hydroxide (1 M) solutions. The solution was further ozonated in a semi-batch gas-liquid reactor (Figure 1) equipped with a porous diffuser until the gas-liquid equilibrium was reached. An ozone flow-rate of $50 \text{ NL}\cdot\text{h}^{-1}$ with an inlet ozone gas concentration around $50\text{-}60 \text{ g}\cdot\text{Nm}^{-3}$ (depending on the solution pH) was produced using an ozone generator (BMT 803N, Germany) fed with oxygen gas (Gaz Liquide, France). These conditions enabled to reach a dissolved ozone concentration at equilibrium around 10 ppm at equilibrium (after 30 min). The dissolved ozone concentration at equilibrium was quantified by the indigo method on at least three samples withdrawn directly in the gas-liquid reactor. The temperature was kept constant at $20 \pm 1^\circ\text{C}$ using a thermostatic bath. When the gas-liquid equilibrium was reached inside the reactor, a membrane pump (KNF, Germany) was turned on to feed the recirculation line while the ozone equilibrium was maintained in the gas-liquid reactor. The recirculation line contained a float-type flowmeter (Brooks Sho-Rate, USA), a dissolved ozone analyzer (ATI Q45/H, USA) to check the dissolved ozone concentration and a 500 mL flask containing the membrane coupon ($4.5 \text{ cm} \times 4.5 \text{ cm}$). The flow-rate was kept constant at 18 L h^{-1} in the recirculation line. After 1 h of exposure (corresponding to an applied ozone dose at the flask inlet of 180 mg for each experiment), the ozone generator was turned off allowing to quickly strip the dissolved ozone in solution in the gas-liquid reactor. When the amount of dissolved ozone became negligible (*i.e.* after a few minutes), the pump was turned off and the system was drained to collect the ozonated membranes. The latter were then thoroughly rinsed with DI water and stored at 4°C until characterization.

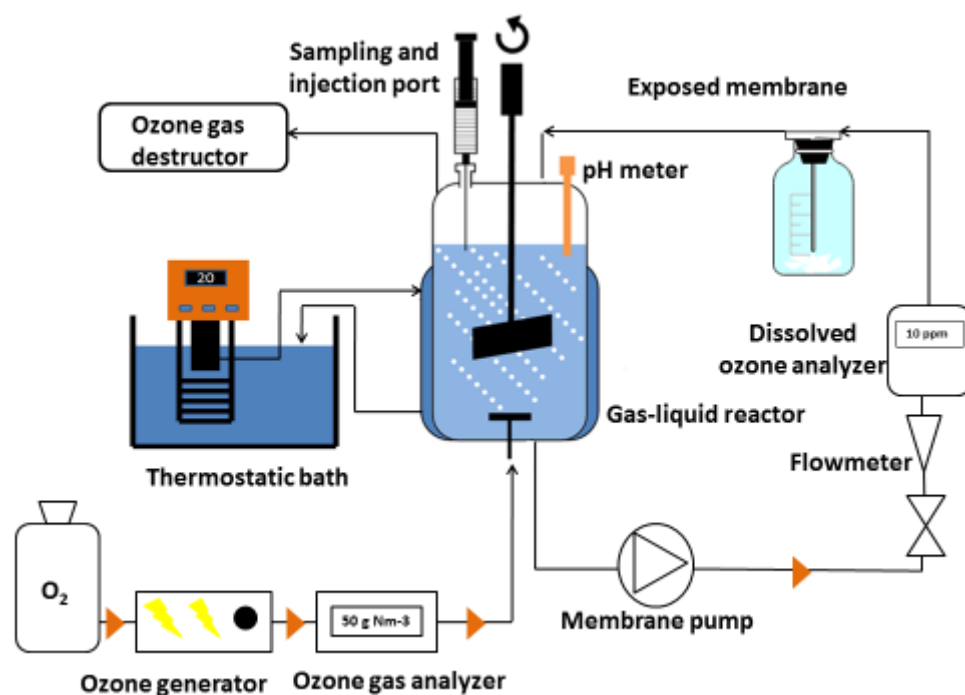


Figure 1. Experimental set-up for membrane ozonation.

It is worth mentioning that ozonation in aqueous solutions involves reactions with either molecular ozone and with reactive oxygen species, mainly hydroxyl radicals HO^\bullet but also O_2^\bullet , HO_2^\bullet , etc.[16]. A complex chain of radicals is formed in the degradation of ozone, which depends on the medium. For instance, in pure water, the ozone decomposition is mainly initiated by the hydroxyl anion (see Supplementary Information). Accordingly, working at acidic pH allows to slow down the ozone decomposition (around 5 times compared to at pH 7 [40]) and the radical generation. At neutral pH, the ozone decomposition is faster and concomitant with a significant radical generation. Consequently, a higher exposition to molecular ozone and a lower exposition to radicals occurs at pH 3 than at pH 7 and *vice versa*. However, it is not possible to completely avoid radicals at pH 3 (except using a radical scavenger) and to avoid molecular ozone at pH 7. Indeed, the hydraulic residence time in the vessel containing the membrane was less than 2 minutes and was thus lower than the typical reaction time corresponding to the ozone decomposition. For example, at pH 7, a first-order reaction rate constant relative to the ozone decomposition of around 0.001 s^{-1} is expected [40]. It means that the ozone half-life time would be higher than 10 minutes. Thus, even if the membrane presence is likely to decrease slightly the ozone life-time (due to ozone-polymer

reactions), molecular ozone was then still present in solution at pH 7 at the flask outlet, showing that both reactions with radicals and molecular ozone can be potentially involved.

2.4 Membrane characterization

2.4.1. Zeta potential

Membrane zeta potential was determined using a SurPASS electrokinetic analyzer (Anton Paar GmbH, Graz) equipped with Ag/AgCl electrodes and an adjustable-gap cell. The streaming current technique was preferred over the streaming potential to avoid any potential contribution of the electrical conduction through the membrane support [41,42]. Measurements were conducted at room temperature with 0.001 M KCl background solutions in the pH range 3-9 (the pH was adjusted with 0.05M HCl and KOH solutions). The distance between the membrane samples (dimensions: 2 cm × 1 cm) was set to $100 \pm 5 \mu\text{m}$.

2.4.2. Attenuated Total Reflectance- Fourier Transform Infrared (ATR-FTIR)

In order to characterize chemical modifications induced by ozonation, the ATR-FTIR spectra of membranes were recorded using a PerkinElmer Spectrum™ 100 FTIR spectrometer. Samples were measured in attenuated total reflectance (ATR) mode with a diamond crystal (single reflection; incidence angle: 45°). Each spectrum was averaged from 25 scans in the range $600\text{--}3700 \text{ cm}^{-1}$ at a resolution of 2 cm^{-1} . Membrane samples were vacuum-dried for 72 h prior to analysis.

2.4.3. X-ray photoelectron spectroscopy (XPS)

XPS spectroscopy was performed with a Kratos Analytical spectrometer (Shimadzu) employing the monochromatic aluminum $K\alpha$ radiation as X-ray excitation source (1486 eV). Membrane samples were mounted on a sample holder with adhesive tape and kept overnight at high vacuum in the preparation chamber before they were transferred to the analysis chamber of the spectrometer. CasaXPS software was used for acquisition and data analysis.

2.4.4. Scanning electron microscopy (SEM)

Membrane morphology was characterized by scanning electron microscopy (SEM) with a JOEL JDM 7100F microscope. Membrane samples were coated with an Au/Pd alloy prior to analysis.

2.4.5. Atomic Force Microscopy (AFM)

Topography of membrane surfaces was characterized with an NTEGRA AFM microscope. Imaging was performed in tapping mode with an etched silicium probe (spring constant: 1.6N/m, resonant frequency: 50–80 kHz). Scanning area was $10\mu\text{m}\times 10\mu\text{m}$. Gwyddion software was used to determine roughness parameters.

2.4.6. Water contact angle

Contact angles were measured by the sessile-drop method using a DIGIDROP GBX-DS apparatus. A syringe was used to deposit DI water droplets with controlled size. Contact angles were determined by means of a video capture system and the Windrop++ software. The reported contact angles are the average of 20 measurements performed at different locations on the membrane surface (errors are indicated by standard deviations). Measurements were performed at room temperature. Membrane samples were vacuum-dried for 72 h prior to measurements.

2.4.7. Pure water permeability

Permeation tests were performed with a Millipore stirred cell (dead-end mode) and 300 mL of DI water. The active surface area of membrane samples was 32.5 cm^2 . Experiments were carried out at various working pressures ranging from 1 to 5 bar and at room temperature. Permeability values are given at 20°C after viscosity correction. Prior to measurements, the membranes were first compacted at 5 bars with DI water for at least 4 h until a constant flux was reached.

3. Results and discussion

3.1. Polyethersulfone (PES) membrane

ATR-FTIR spectra of NP10 membranes before after exposure to ozone are shown in Figure 2. The bands located at 1104 cm^{-1} , 1485 cm^{-1} , 1576 cm^{-1} (aromatic rings), 1147 cm^{-1} , 1165 cm^{-1} , 1296 cm^{-1} , 1321 cm^{-1} (sulfone) and 1238 cm^{-1} (ether) are characteristics of PES [43]. Furthermore, the spectrum of the virgin membrane showed an absorption band at 1668 cm^{-1} that was associated with the amide band (stretching vibration of the C=O double bond of the amide group) of the PVP additive [44].

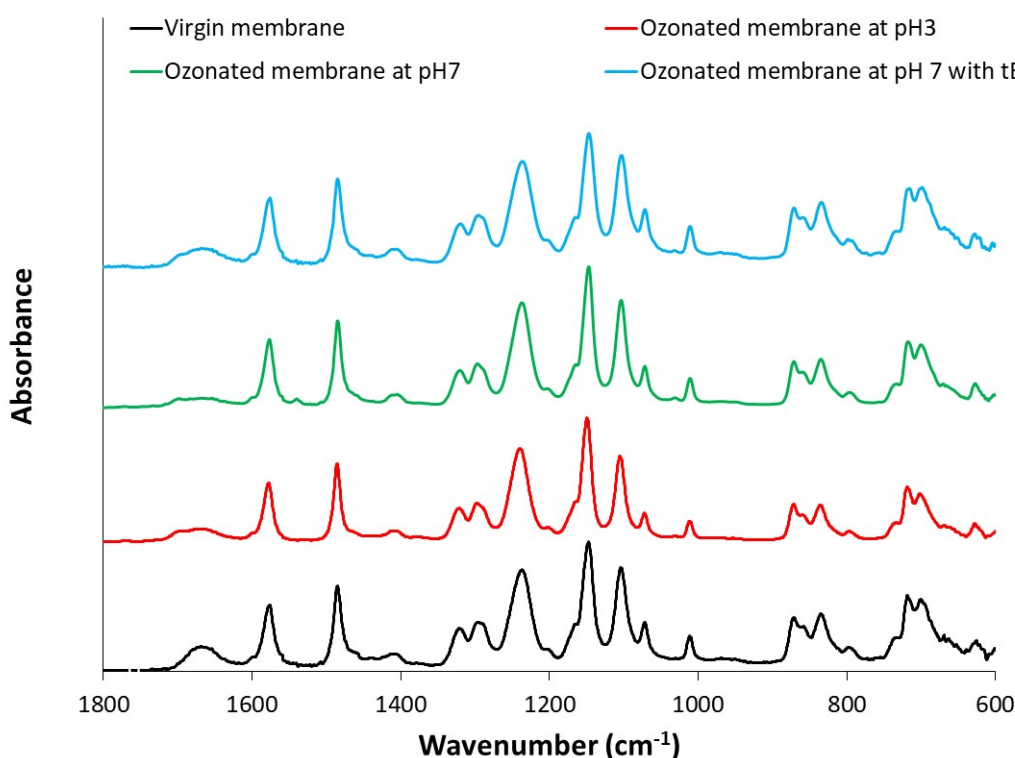
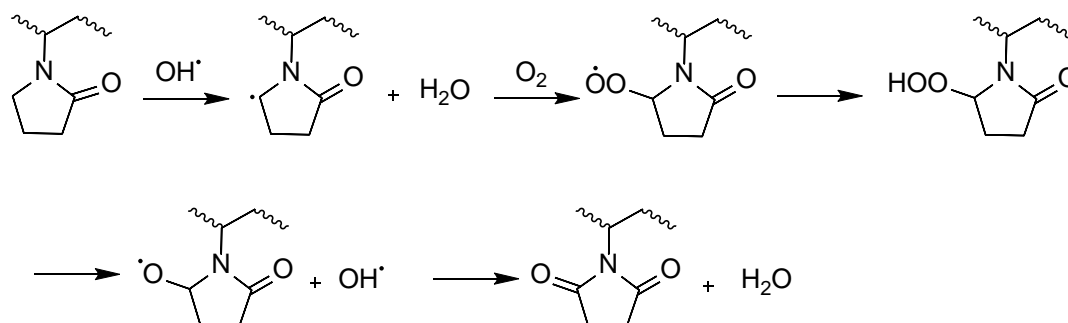


Figure 2. ATR-FTIR spectra of NP10 membranes (virgin membrane and ozonated membranes at pH 3 and 7).

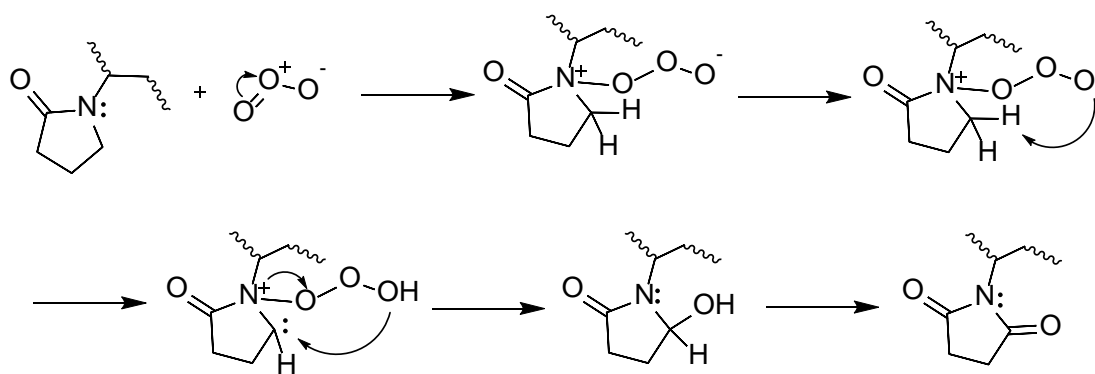
The broadening and decrease in intensity of the amide band of PVP was observed for ozonated membranes, whatever the pH. The oxidation of PVP by hydroxyl radicals (HO^\bullet), leading to the formation of succinimide groups (scheme 1), has been reported after photo-oxidation [45], thermo-oxidation [46] or exposure to sodium hypochlorite under alkaline conditions [46,47]. Succinimides (cyclic imides) are characterized by two bands located at 1700 and 1770 cm^{-1}

[48]. However, Pruhlo et al. reported that the band at 1700 cm^{-1} could be masked so that only a broadening of the initial amide band could occur [46]. Conversely, Hanafi et al. observed the appearance of a shoulder at 1700 cm^{-1} but the band at 1770 cm^{-1} was only detected under very harsh ageing conditions by sodium hypochlorite (400 ppm free chlorine at pH 8 for at least 20 days) [47]. Figure 2 shows qualitatively similar results as those reported by Hanafi et al. with a shoulder at 1700 cm^{-1} after membrane ozonation but no band at 1770 cm^{-1} .



Scheme 1. Formation of succinimides resulting from the attack of PVP by hydroxyl radicals (adapted from [46]).

Interestingly, the shoulder at 1700 cm^{-1} also appeared on the spectrum of the ozonated membrane at pH 3 for which the amount of free radicals generated should be low. It means that molecular ozone might be also able to attack PVP and that succinimides might also be formed by a non-radical mechanism (scheme 2). That was confirmed by additional ozonation experiments performed at pH 7 in the presence of tertibutanol (tBuOH), introduced at 0.01 M, acting as a free radical scavenger. The electrophilic O_3 reacts primarily with the nitrogen atom of nucleophilic organic nitrogen compounds with rate constants depending on the partial charge of the nitrogen atom. Our results are in line with those of Tachibana et al. who studied the reactions of various pyrrolidone derivatives with ozone at pH 2 and identified the formation of N-alkyl succinimide by both gas chromatography – mass spectroscopy and ^{13}C nuclear magnetic resonance [49].



Scheme 2. Formation of succinimides resulting from the electrophilic attack of PVP by molecular ozone (adapted from [49]).

The characteristic bands of PES were not impacted after ozonation of the NP10 membrane, thus suggesting that PES was not degraded by ozone (under the exposure conditions of our study). It has been well-established that ozone reacts with electron-rich aromatic compounds [16]. Aromatic rings of PES appeared, however, quite resistant. It results from the strong electron-withdrawing effect of the neighboring sulfone group (SO_2), which decreases the electron density on the aromatic ring. Hydroxylation of PES aromatic rings resulting from substitution of hydrogen by HO^\bullet has been reported in the literature with the appearance of an additional IR band in the range $1030 - 1035 \text{ cm}^{-1}$ [46,47]. Besides, the cleavage of the C-S bond after exposure of PES membranes to sodium hypochlorite [50] or hydrogen peroxide [51] has been reported, with the formation of sulfonic acid groups ($-\text{SO}_3\text{H}$) and the appearance of an IR band in the same region as for hydroxylation of PES aromatic rings [50]. Only a tiny band seemed to emerge around 1030 cm^{-1} for NP10 membranes exposed to ozone at pH 7 (see Figure 2). The above-mentioned results enabled us to conclude that the degradation of PES, if any, was negligible. The fairly good resistance of PES was confirmed by additional ozonation experiments performed with PES powder (see Supplementary Information).

Table 2 shows the elemental composition obtained by XPS for both virgin and ozonated NP10 membranes. As sulfur (S) and nitrogen (N) atoms are contained only in PES and PVP, respectively, the N/S atomic ratio can be considered as a direct evaluation of the fraction of PVP present at the membrane extreme surface [52]. This ratio remained constant (0.39 ± 0.01) after exposure to ozone, which indicates that the degradation products of PVP remained “trapped” into the PES matrix and were not released from the membrane. A possible reason is that PVP can undergo a cross-linking process under action of ozonation as it has been reported

in several studies dealing with advanced oxidation processes [45,53]. Indeed, Wienk et al. demonstrated by means of steric exclusion chromatography that PVP-chain scission occurred upon radical oxidation [54]. The latter leads to the formation of macro alkyl radicals by the abstraction of a hydrogen atom from the PVP backbone or the pyrrolidone ring [45]. These macro radicals are further likely to form covalent bonds in an intermolecular cross-linking process [55]. Suave et al. notably attributed the formation of hydro gel by PVP after TiO₂/O₃/UV treatments performed in the pH range 3 - 7 to their combination of such macro alkyl radicals [53].

Table 2. Elemental composition (atomic percentages) at the surface of NP10 membranes before and after exposure to ozone.

	S 2p(%)	C 1s(%)	N 1s(%)	O 1s(%)	Ratio N/S
Virgin membrane	6.7	62.2	2.5	29.8	0.38
Ozonated at pH3	8.3	56.8	3.3	31.4	0.40
Ozonated at pH7	5.6	64.4	2.2	27.6	0.39

Figure 3 shows the pH dependence of the zeta potential for NP10 membranes before and after ozonation at pH 3 and 7. The virgin membrane exhibited electrokinetic features in good agreement with those reported in the literature for PES/PVP membranes, *i.e.* a negative zeta potential over a wide range of pH and an isoelectric point around pH 3 [44,56]. After exposure to ozone, membranes had a more negative zeta potential, whatever the pH at which ozonation was carried out. This indicates a change in the surface chemistry of ozonated membranes. The more negative zeta potentials of ozonated membranes can be due to the degradation products of PVP such as e.g. succinimides. It has indeed been established that succinimides easily undergo hydrolysis leading to the opening of the pyrrolidone ring and the formation of carboxylic acid groups (Scheme 3). It is worth noting that even though the zeta potential of ozonated membranes was found to be substantially more negative than the virgin membrane, the membrane isoelectric point (iep) was only weakly impacted, with a slight shift towards more acid pH. Indeed, extrapolation of the electrokinetic data reported in Figure 3 indicates that the shift of the membrane iep after ozonation was less than 0.5. This finding confirms the conclusion drawn from ATR-FTIR analysis about the fairly good resistance of PES. Indeed, a non-negligible cleavage of C-S bonds in PES, and the resulting formation of sulfonic acid

groups (strong acids), should have resulted in a substantial shift or even disappearance of the membrane iep as it was reported by Hanafi et al. for PES membranes exposed to sodium hypochlorite [44,47].

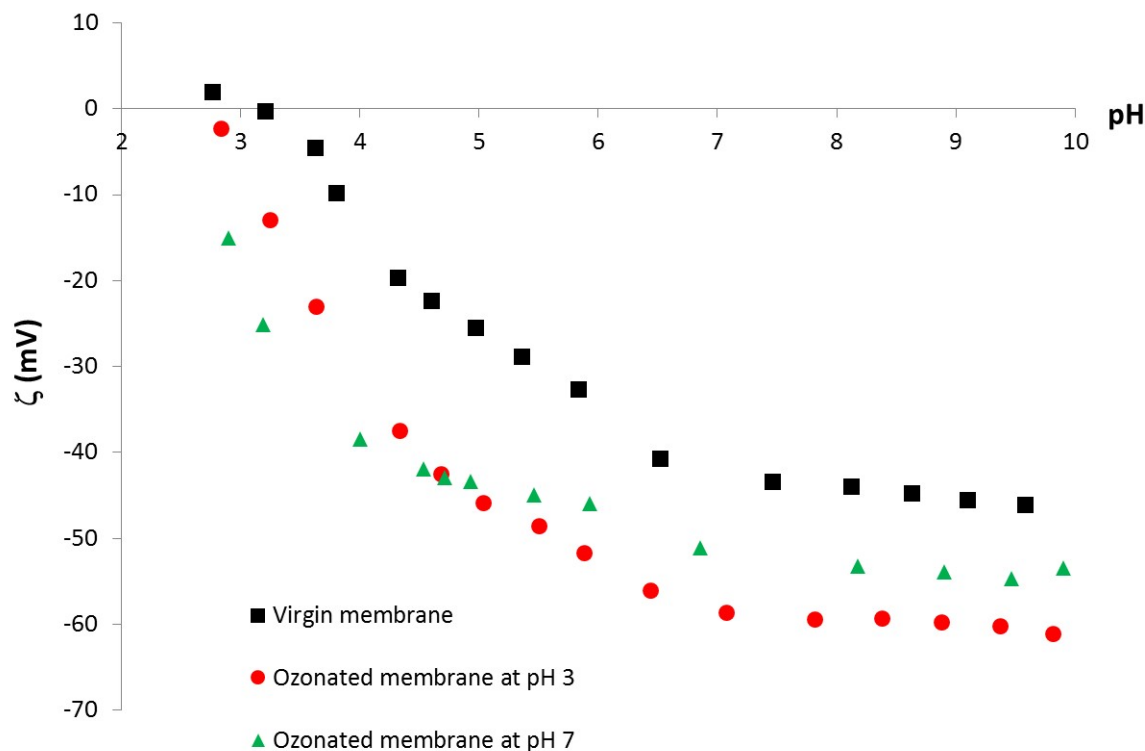
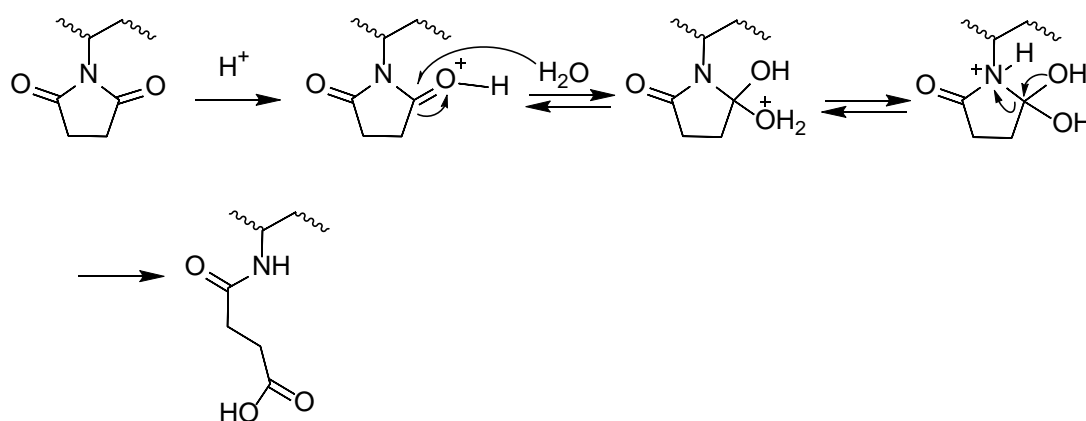


Figure 3. pH dependence of the zeta potential (ζ) of NP10 membranes before and after exposure to ozone.



Scheme 3. Hydrolysis mechanism of succinimides (adapted from [54]).

Water contact angles values determined with virgin and ozonated membranes are presented in Table 3. After ozonation, NP10 membranes exhibited lower contact angle values than the virgin

membrane. It indicates an increase of surface hydrophilicity, which is consistent with the formation of carboxylic acids as end products of PVP degradation.

Table 3. Water contact angle of NP10 membranes before and after exposure to ozone.

Virgin membrane	Ozonated membrane at pH 3	Ozonated membrane at pH 7
$92 \pm 3^\circ$	$61 \pm 3^\circ$	$77 \pm 2^\circ$

SEM and AFM were used to evaluate the influence of ozone on NP10 membrane microstructure. The microscale morphology revealed by SEM indicated a rather dense surface for all membranes (Figure 4). No significant modification of the morphology was observed after exposure of NP10 membranes to ozone. However, AFM revealed that the surface of ozonated membranes was substantially rougher compared to the virgin membrane (Table 4). As discussed above, ozonated PVP can cross-link by recombination of macro alkyl radicals. Such a cross-linking process might induce conformation change of polymer chains, resulting in an increase in surface roughness. It might have a detrimental effect on membrane performance as an increase in surface roughness increases is likely to make the membrane more prone to fouling [57] due to reduced repulsive energy barrier compared to smooth surfaces [58].

Table 4. Roughness of NP10 membranes before and after exposure to ozone.

R_a : average roughness; R_{rms} : root-mean-square roughness.

	Virgin membrane	Ozonated at pH3	Ozonated at pH7
R_a (nm)	47.5	105.2	166.2
R_{rms} (nm)	66.4	137.7	246.2

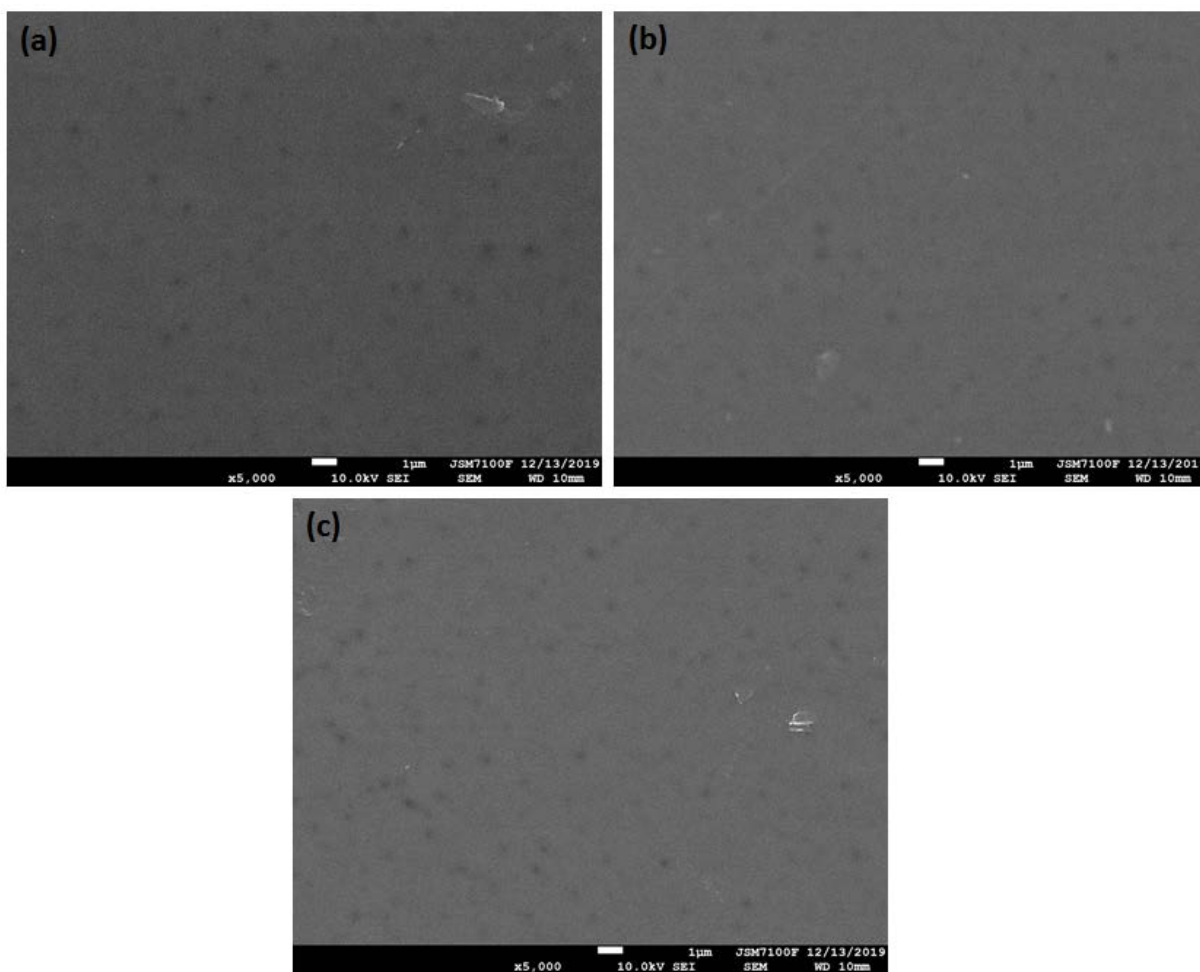


Figure 4. SEM images of NP10 membranes before and after ozonation (scale bar: 1 μm). (a) Virgin membrane; (b) Ozonated membrane at pH 3; (c) Ozonated membrane at pH7.

Figure 5 shows the pure water permeability (L_p) of NP10 membranes before and after ozone treatment. Strikingly, L_p was found to decrease after exposure to ozone unlike what was reported for cellulose acetate membranes [39]. This finding could be explained by cross-linking reactions underwent by PVP during ozonation, which are likely to make the membrane matrix a bit denser. Pure water permeability appeared to be a bit more impacted for the membrane ozonated at pH 7, which is probably related to the favored decomposition of ozone and the greater amount of HO^\bullet produced at higher pH. It should be stressed, however, that the drop of L_p did not exceed 25 %.

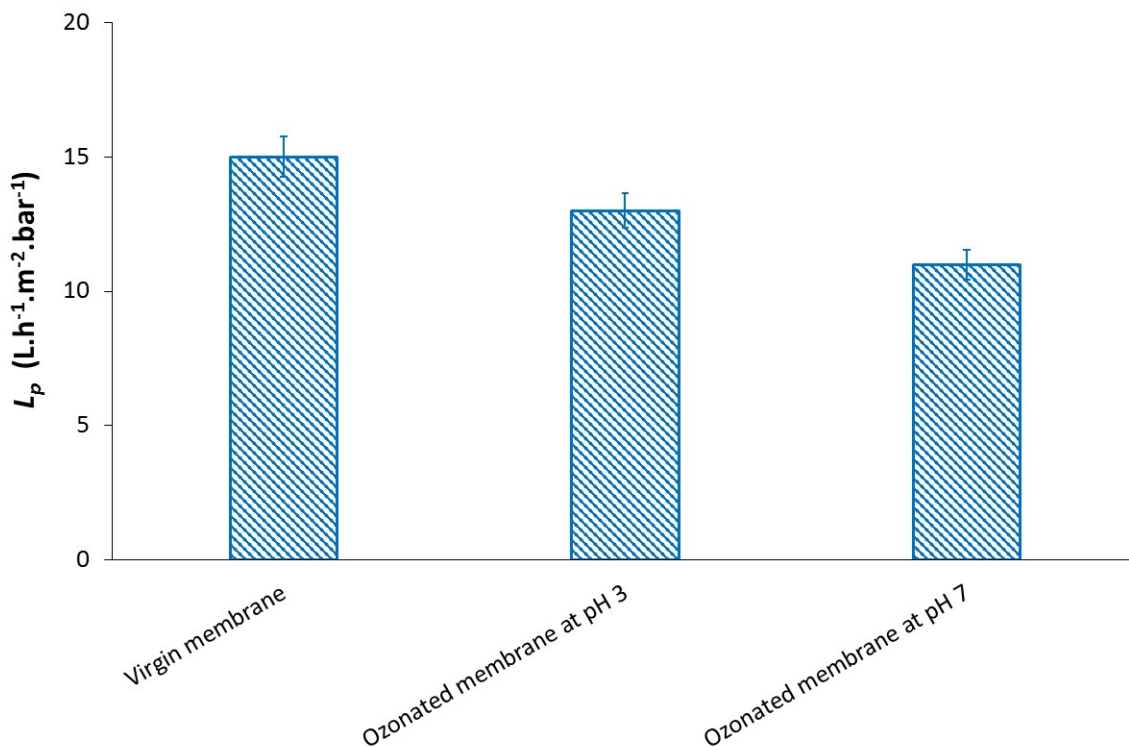


Figure 5. Pure water permeability (L_p) of NP10 membranes before and after ozonation.

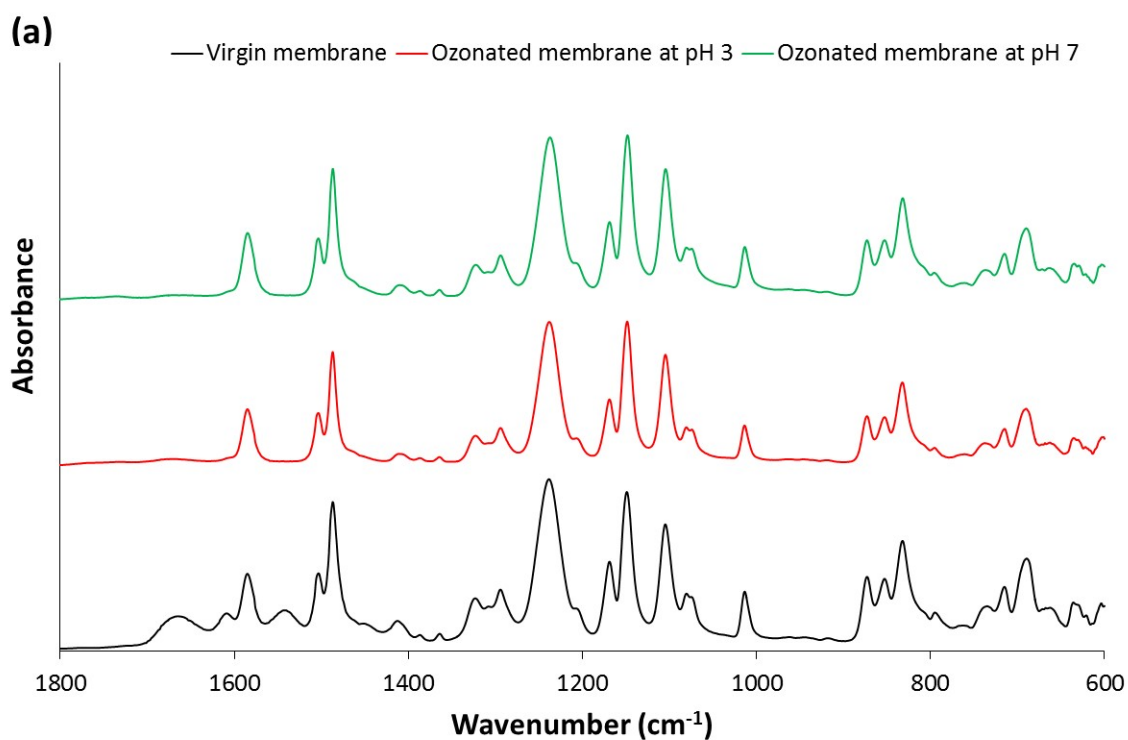
3.2. Polyamide (PA) membranes

Figure 6 shows the ATR-FTIR spectra of NF90 and NF270 membranes before after exposure to ozone. Both membranes are TFC PA membranes obtained by interfacial polymerization on a PSf microporous layer and a macroporous polyester support. NF90 is a fully aromatic PA membrane prepared from TMC and MPD while the monomers used to synthesize the active layer of the NF270 semi-aromatic membrane are TMC and PIP [59].

The characteristic bands of fully aromatic PA membranes are (see the ATR-FTIR spectrum of the virgin NF90 membrane in Figure 6a) (i) the amide I band (1663 cm^{-1}) assigned to C=O stretching, C–N stretching, and C–C–N deformation vibration in a secondary amide group, (ii) the amide II band (1541 cm^{-1}) assigned to N-H in-plane bending and N-C stretching vibration of a secondary amide group, and (iii) the band at 1609 cm^{-1} which is associated with aromatic amides (N-H deformation vibration and C=C ring stretching vibration) [60]. Whatever the ozonation pH, the characteristic bands of the NF90 membrane disappeared after exposure to ozone, with only a shoulder remaining at 1609 cm^{-1} . These results highlight the significant degradation of the NF90 membrane. Furthermore, it can be drawn from results shown in Figure 6a that both molecular ozone and hydroxyl radicals contributed to NF90 membrane attack. The

electrophilic O_3 reacts primarily with the nitrogen atoms of PA membranes. Both the secondary amides and the terminal primary amines of the NF90 membrane were therefore attacked by molecular ozone, with a faster kinetic for amines as the oxygen atom in amide group weakens the electron density on the nitrogen atom [17]. A severe degradation of the aromatic rings of NF90 membrane also occurred as revealed by the almost complete disappearance of the band at 1609 cm^{-1} . It should be stressed that, compared to PES, the aromatic rings of PA are less resistant to ozone attack because they are not protected by the strong electron-withdrawing effect of the sulfone group present in PES.

The disappearance of the characteristic band of the NF 270 semi-aromatic PA membrane, *i.e.* the amide I band located at 1630 cm^{-1} [59], was observed after ozonation at both pH 3 and 7, thus indicating a substantial degradation of the NF270 membrane too (Figure 6b). It was accompanied by the appearance of a new band located at 1725 cm^{-1} , which is associated with stretching of carbonyl groups in ketones [61,62].



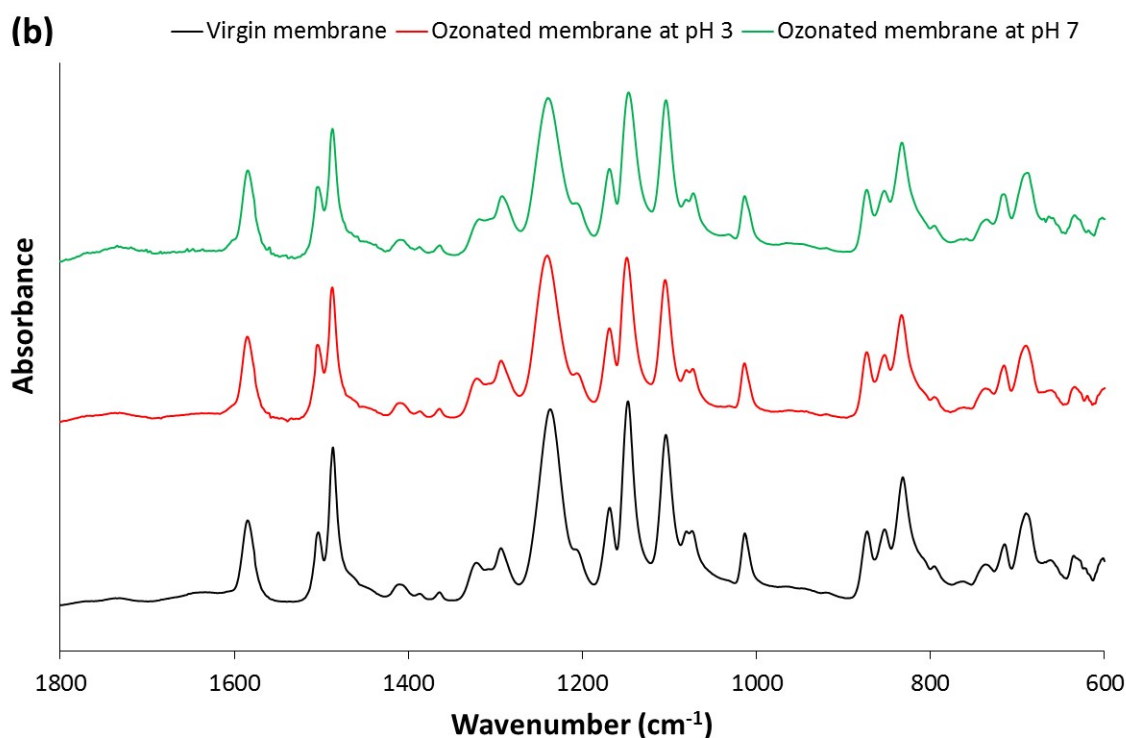
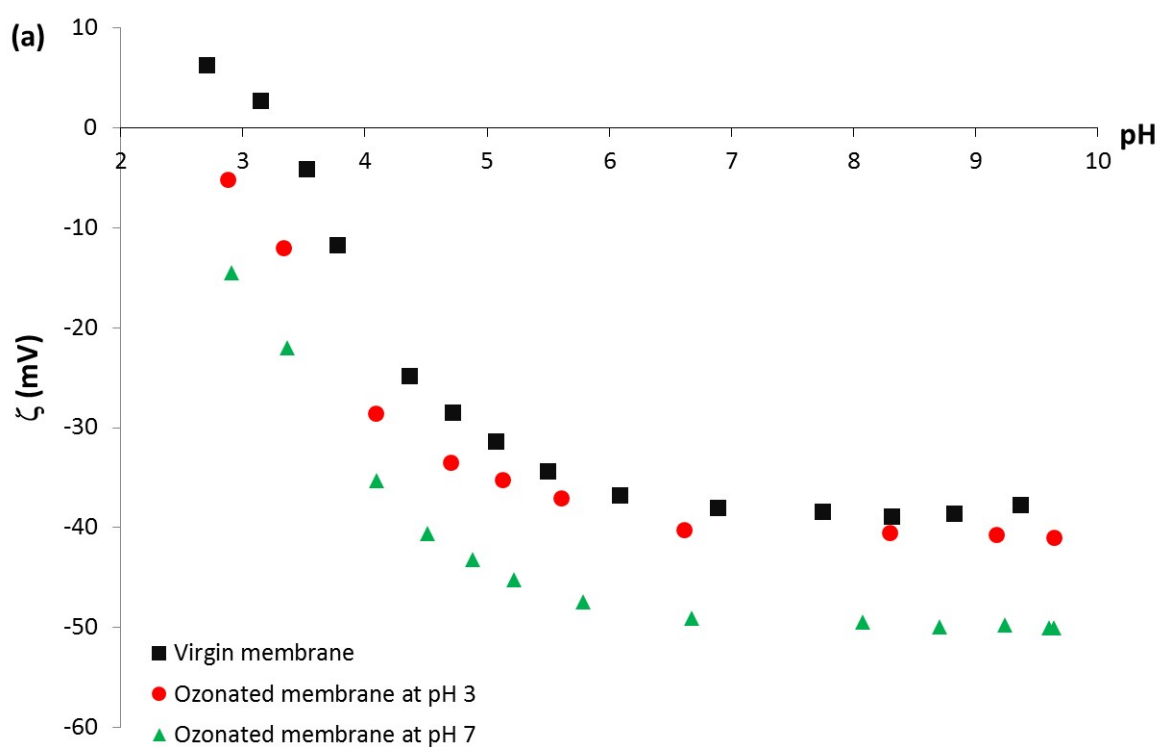


Figure 6. ATR-FTIR spectra of TFC PA membranes (virgin membranes and ozonated membranes at pH 3 and 7). (a) NF90; (b) NF270.

The zeta potential of both TFC PA membranes (NF90 and NF270) before and after ozonation is reported in Figure 7. Both membranes were found more negatively charged after ozonation. Direct attack by molecular ozone is a selective reaction which, in many cases, results in the formation of carboxylic acids as end products [63]. For instance, the aromatic rings of both NF90 and NF270 membranes can be attacked by ozone via a Criegee-like mechanism [64] with the formation of an ozonide and its breakdown leading to the formation of carboxylic acid groups [17]. This mechanism most likely contributed to the more negative surface charge density of NF90 and NF270 membranes after ozonation. Interestingly, the zeta potential of the NF90 membrane was found to be more negative for the membrane that underwent ozonation at pH 7 (Figure 7a) whereas almost no impact of the ozonation pH was observed for the NF270 (Figure 7b). Compounds containing an amine group lose their ozone reactivity upon protonation because amine protonation limits the electrophilic attack of O_3 by decreasing the electronic density on the nitrogen atom [17]. As stated above, NF90 and NF270 are synthesized from MPD (aromatic amine) and PIP (non-aromatic amine), respectively. MPD is less basic than PIP because the aromatic ring of MPD allows conjugation between the lone electron pair of the nitrogen atom and the π electrons of the aromatic ring. Terminal amines of the NF90 membrane

are therefore likely to be protected against ozone when ozonation is performed at pH 3 but they can be degraded when ozonated at pH 7 (the pK_a of the MPD^+/MPD system is about 5.1 at 25°C). That may explain why the NF90 membrane ozonated at pH 7 had a more negative charge and a lower iep than the membrane ozonated at pH 3 (Figure 7a). In contrast, the terminal amines of the NF270 membrane are expected to be protonated, and thus protected from ozone, at both pH 3 and 7 (the pK_a of the PIP^+/PIP system is about 9.8 at 25°C), which may explain why both the zeta potential and iep of the NF270 membrane were found to be only weakly impacted by the ozonation pH (Figure 7b).



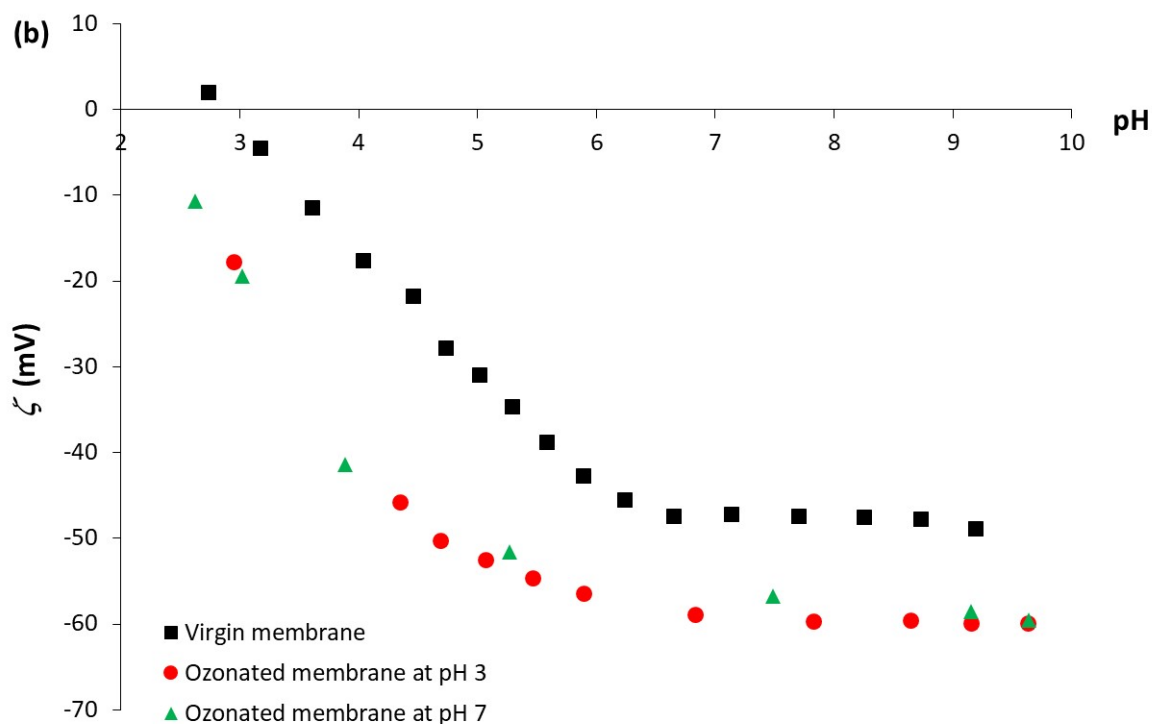


Figure 7. pH dependence of the zeta potential (ζ) of TFC PA membranes before and after exposure to ozone. (a) NF90; (b) NF 270.

Although the pristine NF90 and NF270 membranes had different iep (3.3 and 3.0, respectively), it is worth noting that their iep turned out to be identical (around pH 2.3) after ozonation. These results, together with the ATR-FTIR analysis (Figure 6), suggest that a substantial part of the PA active layer was destroyed by ozonation and might indicate that a substantial part of the surface of the ozonated membranes was actually made up of the (underlying) PSf layer. This argument is supported by SEM images (Figures 8 and 9). For the NF90 membrane, the typical ridge-and-valley morphology of fully aromatic PA membranes (Figure 8a) was found to be erased after ozonation (Figures 8b and 8c), this being more pronounced for the membrane ozonated at pH 7 for which HO^\bullet radicals resulting from ozone decomposition participated in the membrane degradation. The virgin semi-aromatic NF270 membrane was found to have a much smoother surface (Figure 9a) than the fully-aromatic NF90 membrane as it was already reported in the literature [59]. After ozonation, some areas of the NF270 membrane surface showed significant cracks as shown in Figures 9b and 9c, thus revealing significant damage to the membrane structure. It has to be kept in mind, however, that the formation of these cracks might result from SEM operating conditions (i.e. high vacuum) and not directly from ozonation itself. This argument is supported by the fact that the impact of ozonation on the membrane

permeability was found greater for the NF90 than for the NF270 (see below) despite the fact that no crack was observed on the NF90 active layer. It must be stressed, however, that no crack was observed at the surface of the pristine NF270 membrane, thus indicating that the formation of cracks resulted from the embrittlement of the active layer during ozonation.

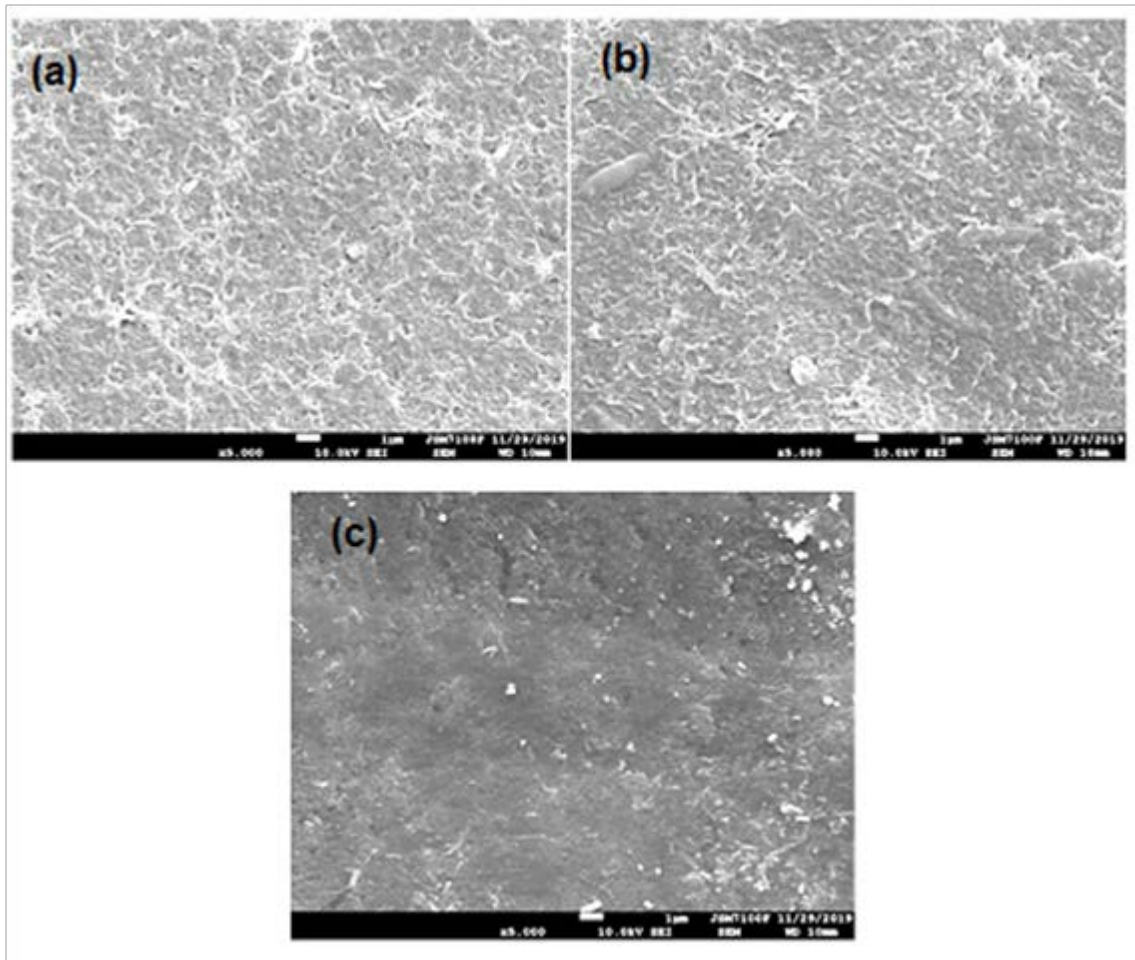


Figure 8. SEM images of NF90 membranes before and after ozonation (scale bar: 1 µm). (a) Virgin membrane; (b) Ozonated membrane at pH 3; (c) Ozonated membrane at pH7.

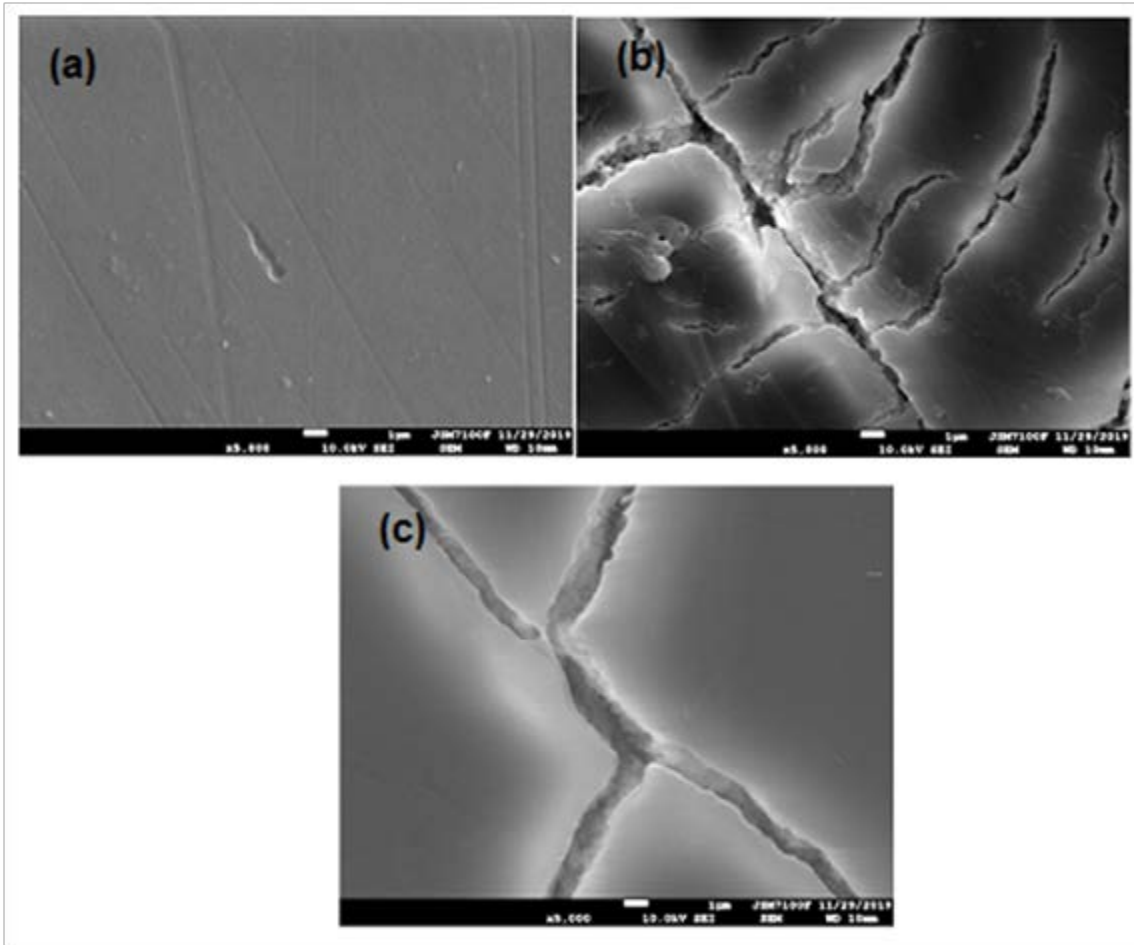


Figure 9. SEM images of NF270 membranes before and after ozonation (scale bar: 1 μm). (a) Virgin membrane; (b) Ozonated membrane at pH 3; (c) Ozonated membrane at pH 7.

Water contact angles values determined with virgin and ozonated NF 270 and NF90 membranes are collected in Table 5. The contact angle measured with the virgin NF90 membranes was found to be $67 \pm 3^\circ$, in fairly good agreement with data reported in the literature [65–67]. The surface of the NF270 membrane was found to be much more hydrophilic than the NF90 membrane, with a water contact angle of $23 \pm 3^\circ$ (it is worth mentioning that values reported in the literature for this membrane are very scattered, ranging from 10° to more than 60° [7,66,68–70]). After ozonation, NF270 membranes exhibited much higher contact angles (up to 62° for the membrane ozonated at pH 7), thus indicating a less hydrophilic surface. No clear tendency was obtained with the NF90 membrane. Strikingly, the standard deviation on the contact angle measurements was found to increase dramatically for both membranes after ozonation (Table 5). This is most likely the result of the heterogeneous degradation of the membrane surfaces, as shown in the SEM images (Figures 8 and 9). It is worth mentioning that the results shown in Table 5 are also compatible with the hypothesis that part of the PSf layer appeared on the surface

of ozonated membranes due to partial elimination of the PA active layer, as water contact angle of PSf has usually been reported in the range 75-90° [71–74].

Table 5. Water contact angle of NF 90 and NF 270 membranes before and after exposure to ozone.

NF90			NF270		
Virgin membrane	Ozonated membrane at pH 3	Ozonated membrane at pH 7	Virgin membrane	Ozonated membrane at pH 3	Ozonated membrane at pH 7
67 ± 3°	55 ± 7°	65 ± 9°	23 ± 3°	62 ± 13°	41 ± 5°

Figure 10 shows the pure water permeability (L_p) of NP90 and NF270 membranes before and after ozone treatment. In contrast to the results obtained for the NP10 PES membrane, a significant increase in the permeability of both PA membranes was observed, this increase being even more marked for the NF90 membrane. This indicates that the active layer of the NF90 membrane underwent greater degradation than that of the NF270 membrane. In both cases, a greater impact of ozonation on hydraulic permeability was observed at pH 7 than pH 3, which is explained by the additional action of hydroxyl radicals at pH 7 due to the faster decomposition of ozone. After ozonation at pH 7, the hydraulic permeability of the NF270 and NF90 membranes was found to increase by ~80 % and ~500 %, respectively. Such a dramatic increase of L_p supports the argument mentioned above about the partial removal of the active layer of TFC PA membranes.

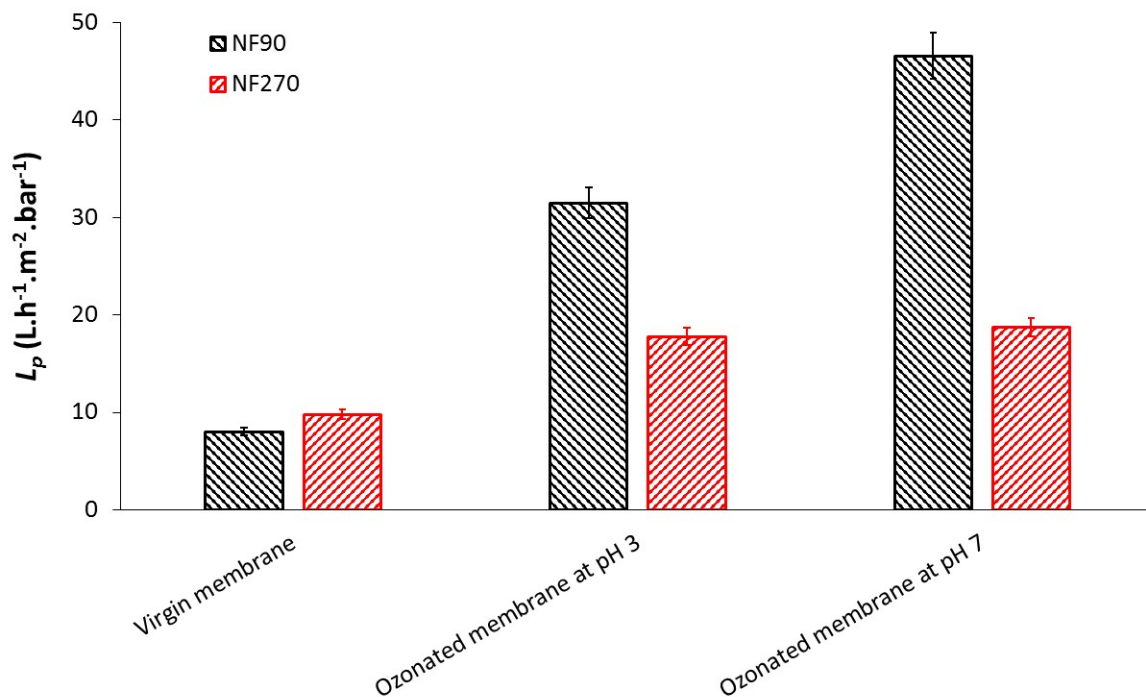


Figure 10. Pure water permeability (L_p) of NF90 and NF270 membranes before and after ozonation.

4. Conclusion

The resistance of PES-based (NP10) and PA (NF90 and NF270) nanofiltration membranes to ozone was investigated. Under the exposure conditions of this study (10 ppm of dissolved ozone at pH 3 and 7 for 1h), no significant degradation of PES was observed, which can be explained in part by the good resistance of its aromatic rings protected from electrophilic attack by the presence of strongly electron-withdrawing sulfone groups. Conversely, PVP, which is used as an additive to PES, was substantially degraded by ozone, in particular by the attack and opening of its pyrrolidone ring. A decrease in the pure water permeability of the NP10 membrane, not exceeding 25%, was observed after ozonation, which could result from cross-linking of degraded PVP by recombination of macroradicals. Both PA membranes were extensively degraded by exposure to dissolved ozone but at different levels due to the different chemical composition of their active layer. The most severe damage was observed for the NF90 membrane, which has an active layer containing a higher number of aromatic ring and less basic terminal amines than the semi-aromatic NF270 membrane. Characterization of membranes after exposure to ozone suggested a partial removal of their active layer and the appearance of

the polysulfone sublayer on the membrane surface. Permeability measurements supported this statement since it was observed an increase in flux of up to 80% and 500% for the NF270 and NF90 membranes, respectively. Overall, the degradation of all membranes was somewhat greater at pH 7 than pH 3 due to the faster decomposition of ozone at pH 7 leading to the formation of more free radicals.

Acknowledgements

The Ministry of Higher Education and Scientific Research of Algeria and Campus France are gratefully acknowledged for providing S. Ouali with a Profas B+ grant (954610C). The authors are also grateful to Jean-François Bergamini, Corinne Lagrost, Pierre Largillière, Thierry Pain (Institut des Sciences Chimiques de Rennes), Cristelle Meriadec (Institut de Physique de Rennes) and Jonathan Hamon (Institut des Matériaux Jean Rouxel) for technical assistance. Francis Gouttefangeas is acknowledged for SEM images analyses performed at CMEBA (ScanMAT, University of Rennes 1) which received a financial support from the European Union (CPER-FEDER 2007-2014).

References

- [1] M. Dalwani, G. Bargeman, S.S. Hosseiny, M. Boerrigter, M. Wessling, N.E. Benes, Sulfonated poly(ether ether ketone) based composite membranes for nanofiltration of acidic and alkaline media, *J. Membr. Sci.* 381 (2011) 81–89. <https://doi.org/10.1016/j.memsci.2011.07.018>.
- [2] M. Siddiqui, Membranes for the control of natural organic matter from surface waters, *Water Res.* 34 (2000) 3355–3370. [https://doi.org/10.1016/S0043-1354\(00\)00024-5](https://doi.org/10.1016/S0043-1354(00)00024-5).
- [3] S. Meylan, F. Hammes, J. Traber, E. Salhi, U. Vongunten, W. Pronk, Permeability of low molecular weight organics through nanofiltration membranes, *Water Res.* 41 (2007) 3968–3976. <https://doi.org/10.1016/j.watres.2007.05.031>.
- [4] S. Van Geluwe, L. Braeken, B. Van der Bruggen, Ozone oxidation for the alleviation of membrane fouling by natural organic matter: A review, *Water Res.* 45 (2011) 3551–3570. <https://doi.org/10.1016/j.watres.2011.04.016>.
- [5] Á. de la Rubia, M. Rodríguez, V.M. León, D. Prats, Removal of natural organic matter and THM formation potential by ultra- and nanofiltration of surface water, *Water Res.* 42 (2008) 714–722. <https://doi.org/10.1016/j.watres.2007.07.049>.
- [6] S. Byun, J.S. Taurozzi, V. V. Tarabara, Ozonation as a pretreatment for nanofiltration: Effect of oxidation pathway on the permeate flux, *Sep. Purif. Technol.* 149 (2015) 174–182. <https://doi.org/10.1016/j.seppur.2015.05.035>.
- [7] M. Mänttari, T. Pekuri, M. Nyström, NF270, a new membrane having promising characteristics and being suitable for treatment of dilute effluents from the paper industry, *J. Membr. Sci.* 242 (2004) 107–116. <https://doi.org/10.1016/j.memsci.2003.08.032>.
- [8] R.F. Fibiger, J. Koo, D.J. Forgach, R.J. Petersen, D.L. Schmidt, R.A. Wessling, T.F. Stocker, NOVEL POLYAMIDE REVERSE OSMOSIS MEMBRANES, 4769148, n.d.
- [9] R.F. Fibiger, J. Koo, D.J. Forgach, R.J. Petersen, D.L. Schmidt, R.A. Wessling, T.F. Stocker, NOVEL POLYAMIDE REVERSE OSMOSIS MEMBRANES, 4859384, n.d.
- [10] T.A. Otitoju, A.L. Ahmad, B.S. Ooi, Recent advances in hydrophilic modification and performance of polyethersulfone (PES) membrane via additive blending, *RSC Adv.* 8 (2018) 22710–22728. <https://doi.org/10.1039/c8ra03296c>.
- [11] A. V. Dudchenko, J. Rolf, K. Russell, W. Duan, D. Jassby, Organic fouling inhibition on electrically conducting carbon nanotube-polyvinyl alcohol composite ultrafiltration membranes, *J. Membr. Sci.* 468 (2014) 1–10. <https://doi.org/10.1016/j.memsci.2014.05.041>.
- [12] K. Katsoufidou, S.G. Yiantsios, A.J. Karabelas, Experimental study of ultrafiltration membrane fouling by sodium alginate and flux recovery by backwashing, *J. Membr. Sci.* 300 (2007) 137–146. <https://doi.org/10.1016/j.memsci.2007.05.017>.
- [13] A.S. Jönsson, G. Trägårdh, Fundamental principles of ultrafiltration, *Chem. Eng. Process.* 27 (1990) 67–81. [https://doi.org/10.1016/0255-2701\(90\)85011-R](https://doi.org/10.1016/0255-2701(90)85011-R).
- [14] K. Ibn Abdul Hamid, P.J. Scales, S. Allard, J.-P. Croue, S. Muthukumar, M. Duke, Ozone combined with ceramic membranes for water treatment: Impact on HO radical formation and mitigation of bromate, *J. Environ. Manage.* 253 (2020) 109655. <https://doi.org/10.1016/j.jenvman.2019.109655>.
- [15] F.R.A. dos Santos, C.P. Borges, F.V. da Fonseca, Polymeric Materials for Membrane Contactor Devices Applied to Water Treatment by Ozonation, *Mater. Res.* 18 (2015) 1015–1022. <https://doi.org/10.1590/1516-1439.016715>.
- [16] U. von Gunten, Ozonation of drinking water: Part I. Oxidation kinetics and product formation, *Water Res.* 37 (2003) 1443–1467. [https://doi.org/10.1016/S0043-1354\(02\)00457-8](https://doi.org/10.1016/S0043-1354(02)00457-8).
- [17] C. von Sonntag, U. von Gunten, *Chemistry of Ozone in Water and Wastewater Treatment: From Basic Principles to Applications*, IWA Publishing, 2012. <https://doi.org/10.2166/9781780400839>.

- [18] F.J. Beltran, *Ozone Reaction Kinetics for Water and Wastewater Systems*, CRC Press, 2003.
- [19] J. Hoigné, *Chemistry of Aqueous Ozone and Transformation of Pollutants by Ozonation and Advanced Oxidation Processes*, in: J. Hrubec (Ed.), *Qual. Treat. Drink. Water II*, Springer Berlin Heidelberg, Berlin, Heidelberg, 1998: pp. 83–141. https://doi.org/10.1007/978-3-540-68089-5_5.
- [20] J. Staehelin, J. Hoigne, Decomposition of ozone in water: rate of initiation by hydroxide ions and hydrogen peroxide, *Environ. Sci. Technol.* 16 (1982) 676–681. <https://doi.org/10.1021/es00104a009>.
- [21] J. Staehelin, J. Hoigne, Decomposition of ozone in water in the presence of organic solutes acting as promoters and inhibitors of radical chain reactions, *Environ. Sci. Technol.* 19 (1985) 1206–1213. <https://doi.org/10.1021/es00142a012>.
- [22] M. Park, T. Anumol, J. Simon, F. Zraick, S.A. Snyder, Pre-ozonation for high recovery of nanofiltration (NF) membrane system: Membrane fouling reduction and trace organic compound attenuation, *J. Membr. Sci.* 523 (2017) 255–263. <https://doi.org/10.1016/j.memsci.2016.09.051>.
- [23] W. Yu, T. Liu, J. Crawshaw, T. Liu, N. Graham, Ultrafiltration and nanofiltration membrane fouling by natural organic matter: Mechanisms and mitigation by pre-ozonation and pH, *Water Res.* 139 (2018) 353–362. <https://doi.org/10.1016/j.watres.2018.04.025>.
- [24] S.O. Ganiyu, E.D. van Hullebusch, M. Cretin, G. Esposito, M.A. Oturan, Coupling of membrane filtration and advanced oxidation processes for removal of pharmaceutical residues: A critical review, *Sep. Purif. Technol.* 156 (2015) 891–914. <https://doi.org/10.1016/j.seppur.2015.09.059>.
- [25] N. Rosman, W.N.W. Salleh, M.A. Mohamed, J. Jaafar, A.F. Ismail, Z. Harun, Hybrid membrane filtration-advanced oxidation processes for removal of pharmaceutical residue, *J. Colloid Interface Sci.* 532 (2018) 236–260. <https://doi.org/10.1016/j.jcis.2018.07.118>.
- [26] S. Byun, J.S. Taurozzi, A.L. Alpatova, F. Wang, V.V. Tarabara, Performance of polymeric membranes treating ozonated surface water: Effect of ozone dosage, *Sep. Purif. Technol.* 81 (2011) 270–278. <https://doi.org/10.1016/j.seppur.2011.07.021>.
- [27] Y. Yoon, Y. Hwang, M. Ji, B.-H. Jeon, J.-W. Kang, Ozone/membrane hybrid process for arsenic removal in iron-containing water, *Desalination Water Treat.* 31 (2011) 138–143. <https://doi.org/10.5004/dwt.2011.2372>.
- [28] A.D. Ebner, J.A. Ritter, State-of-the-art Adsorption and Membrane Separation Processes for Carbon Dioxide Production from Carbon Dioxide Emitting Industries, *Sep. Sci. Technol.* 44 (2009) 1273–1421. <https://doi.org/10.1080/01496390902733314>.
- [29] C.O. Lee, K.J. Howe, B.M. Thomson, Ozone and biofiltration as an alternative to reverse osmosis for removing PPCPs and micropollutants from treated wastewater, *Water Res.* 46 (2012) 1005–1014. <https://doi.org/10.1016/j.watres.2011.11.069>.
- [30] P. Liu, H. Zhang, Y. Feng, F. Yang, J. Zhang, Removal of trace antibiotics from wastewater: A systematic study of nanofiltration combined with ozone-based advanced oxidation processes, *Chem. Eng. J.* 240 (2014) 211–220. <https://doi.org/10.1016/j.cej.2013.11.057>.
- [31] T. Fujioka, S.J. Khan, J.A. McDonald, L.D. Nghiem, Ozonation of N-Nitrosamines in the Reverse Osmosis Concentrate from Water Recycling Applications, *Ozone Sci. Eng.* 36 (2014) 174–180. <https://doi.org/10.1080/01919512.2013.866885>.
- [32] A. Azaïs, J. Mendret, E. Petit, S. Brosillon, Influence of volumetric reduction factor during ozonation of nanofiltration concentrates for wastewater reuse, *Chemosphere.* 165 (2016) 497–506. <https://doi.org/10.1016/j.chemosphere.2016.09.071>.
- [33] H. Wang, M. Park, H. Liang, S. Wu, I.J. Lopez, W. Ji, G. Li, S.A. Snyder, Reducing ultrafiltration membrane fouling during potable water reuse using pre-ozonation, *Water Res.* 125 (2017) 42–51. <https://doi.org/10.1016/j.watres.2017.08.030>.
- [34] F. Bu, B. Gao, X. Shen, W. Wang, Q. Yue, The combination of coagulation and ozonation as a pre-treatment of ultrafiltration in water treatment, *Chemosphere.* 231 (2019) 349–356. <https://doi.org/10.1016/j.chemosphere.2019.05.154>.

- [35] C. Mansas, J. Mendret, S. Brosillon, A. Ayril, Coupling catalytic ozonation and membrane separation: A review, *Sep. Purif. Technol.* 236 (2020) 116221. <https://doi.org/10.1016/j.seppur.2019.116221>.
- [36] H. Vatankhah, C.C. Murray, J.W. Brannum, J. Vanneste, C. Bellona, Effect of pre-ozonation on nanofiltration membrane fouling during water reuse applications, *Sep. Purif. Technol.* 205 (2018) 203–211. <https://doi.org/10.1016/j.seppur.2018.03.052>.
- [37] Z. Yin, T. Wen, Y. Li, A. Li, C. Long, Alleviating reverse osmosis membrane fouling caused by biopolymers using pre-ozonation, *J. Membr. Sci.* 595 (2020) 117546. <https://doi.org/10.1016/j.memsci.2019.117546>.
- [38] Y. Goto, K. Kitano, T. Maruoka, M. Yamamoto, A. Konno, H. Horibe, S. Tagawa, Removal of Polymers with Various Chemical Structures using Wet Ozone, *J. Photopolym. Sci. Technol.* 23 (2010) 417–420. <https://doi.org/10.2494/photopolymer.23.417>.
- [39] J. Glater, M.R. Zachariah, S.B. McCray, J.W. McCutchan, Reverse osmosis membrane sensitivity to ozone and halogen disinfectants, *Desalination.* 48 (1983) 1–16. [https://doi.org/10.1016/0011-9164\(83\)80001-0](https://doi.org/10.1016/0011-9164(83)80001-0).
- [40] D. Gardoni, A. Vailati, R. Canziani, Decay of Ozone in Water: A Review, *Ozone Sci. Eng.* 34 (2012) 233–242. <https://doi.org/10.1080/01919512.2012.686354>.
- [41] P. Fievet, M. Sbai, A. Szymczyk, A New Tangential Streaming Potential Setup for the Electrokinetic Characterization of Tubular Membranes, *Sep. Sci. Technol.* 39 (2004) 2931–2949. <https://doi.org/10.1081/SS-200028652>.
- [42] E. Idil Mouhoumed, A. Szymczyk, A. Schäfer, L. Paugam, Y.H. La, Physico-chemical characterization of polyamide NF/RO membranes: Insight from streaming current measurements, *J. Membr. Sci.* 461 (2014) 130–138. <https://doi.org/10.1016/j.memsci.2014.03.025>.
- [43] W.-J. Lau, A.F. Ismail, Effect of SPEEK content on the morphological and electrical properties of PES/SPEEK blend nanofiltration membranes, *Desalination.* 249 (2009) 996–1005. <https://doi.org/10.1016/j.desal.2009.09.016>.
- [44] Y. Hanafi, P. Loulergue, S. Ababou-Girard, C. Meriadec, M. Rabiller-Baudry, K. Baddari, A. Szymczyk, Electrokinetic analysis of PES/PVP membranes aged by sodium hypochlorite solutions at different pH, *J. Membr. Sci.* 501 (2016) 24–32. <https://doi.org/10.1016/j.memsci.2015.11.041>.
- [45] F. Hassouna, S. Therias, G. Mailhot, J.-L. Gardette, Photooxidation of poly(N-vinylpyrrolidone) (PVP) in the solid state and in aqueous solution, *Polym. Degrad. Stab.* 94 (2009) 2257–2266. <https://doi.org/10.1016/j.polymdegradstab.2009.08.007>.
- [46] R. Prulho, S. Therias, A. Rivaton, J.-L. Gardette, Ageing of polyethersulfone/polyvinylpyrrolidone blends in contact with bleach water, *Polym. Degrad. Stab.* 98 (2013) 1164–1172. <https://doi.org/10.1016/j.polymdegradstab.2013.03.011>.
- [47] Y. Hanafi, A. Szymczyk, M. Rabiller-Baudry, K. Baddari, Degradation of Poly(Ether Sulfone)/Polyvinylpyrrolidone Membranes by Sodium Hypochlorite: Insight from Advanced Electrokinetic Characterizations, *Environ. Sci. Technol.* 48 (2014) 13419–13426. <https://doi.org/10.1021/es5027882>.
- [48] X. Zhu, P. Lu, W. Chen, J. Dong, Studies of UV crosslinked poly(N-vinylpyrrolidone) hydrogels by FTIR, Raman and solid-state NMR spectroscopies, *Polymer.* 51 (2010) 3054–3063. <https://doi.org/10.1016/j.polymer.2010.05.006>.
- [49] Y. Tachibana, M. Nogami, Y. Sugiyama, Y. Ikeda, Kinetic and Mechanistic Studies on Reactions of Pyrrolidone Derivatives with Ozone, *Ozone Sci. Eng.* 33 (2011) 470–482. <https://doi.org/10.1080/01919512.2011.615720>.
- [50] F. ThomINETTE, O. Farnault, E. Gaudichet-Maurin, C. Machinal, J.-C. Schrotter, Ageing of polyethersulfone ultrafiltration membranes in hypochlorite treatment, *Desalination.* 200 (2006) 7–8. <https://doi.org/10.1016/j.desal.2006.03.221>.

- [51] M.T. Tsehaye, J. Wang, J. Zhu, S. Velizarov, B. Van der Bruggen, Development and characterization of polyethersulfone-based nanofiltration membrane with stability to hydrogen peroxide, *J. Membr. Sci.* 550 (2018) 462–469. <https://doi.org/10.1016/j.memsci.2018.01.022>.
- [52] B. Pellegrin, E. Gaudichet-Maurin, C. Causserand, Mechano-chemical ageing of PES/PVP ultrafiltration membranes used in drinking water production, *Water Supply*. 13 (2013) 541–551. <https://doi.org/10.2166/ws.2013.056>.
- [53] J. Suave, H.J. José, R.F.P.M. Moreira, Degradation of Polyvinylpyrrolidone by Photocatalytic Ozonation and Evaluation of the Influence of Some Operational Parameters, *Ozone Sci. Eng.* 36 (2014) 560–569. <https://doi.org/10.1080/01919512.2014.894452>.
- [54] I.M. Wienk, E.E.B. Meuleman, Z. Borneman, T. van den Boomgaard, C.A. Smolders, Chemical treatment of membranes of a polymer blend: Mechanism of the reaction of hypochlorite with poly(vinyl pyrrolidone), *J. Polym. Sci. Part Polym. Chem.* 33 (1995) 49–54. <https://doi.org/10.1002/pola.1995.080330105>.
- [55] J.M. Rosiak, P. Ulański, Synthesis of hydrogels by irradiation of polymers in aqueous solution, *Radiat. Phys. Chem.* 55 (1999) 139–151. [https://doi.org/10.1016/S0969-806X\(98\)00319-3](https://doi.org/10.1016/S0969-806X(98)00319-3).
- [56] Y. Kourde-Hanafy, P. Loulergue, A. Szymczyk, B. Van der Bruggen, M. Nachtnebel, M. Rabiller-Baudry, J.-L. Audic, P. Pölt, K. Baddari, Influence of PVP content on degradation of PES/PVP membranes: Insights from characterization of membranes with controlled composition, *J. Membr. Sci.* 533 (2017) 261–269. <https://doi.org/10.1016/j.memsci.2017.03.050>.
- [57] M. Elimelech, Xiaohua Zhu, A.E. Childress, Seungkwan Hong, Role of membrane surface morphology in colloidal fouling of cellulose acetate and composite aromatic polyamide reverse osmosis membranes, *J. Membr. Sci.* 127 (1997) 101–109. [https://doi.org/10.1016/S0376-7388\(96\)00351-1](https://doi.org/10.1016/S0376-7388(96)00351-1).
- [58] E.M.V. Hoek, S. Bhattacharjee, M. Elimelech, Effect of Membrane Surface Roughness on Colloid–Membrane DLVO Interactions, *Langmuir*. 19 (2003) 4836–4847. <https://doi.org/10.1021/la027083c>.
- [59] C.Y. Tang, Y.-N. Kwon, J.O. Leckie, Effect of membrane chemistry and coating layer on physiochemical properties of thin film composite polyamide RO and NF membranes: I. FTIR and XPS characterization of polyamide and coating layer chemistry, *Desalination*. 242 (2009) 149–167. <https://doi.org/10.1016/j.desal.2008.04.003>.
- [60] C.Y. Tang, Y.-N. Kwon, J.O. Leckie, Effect of membrane chemistry and coating layer on physiochemical properties of thin film composite polyamide RO and NF membranes II. Membrane physiochemical properties and their dependence on polyamide and coating layers, *Desalination*. 242 (2009) 168–182. <https://doi.org/10.1016/j.desal.2008.04.004>.
- [61] L. Puro, M. Mänttari, A. Pihlajamäki, M. Nyström, Characterization of Modified Nanofiltration Membranes by Octanoic Acid Permeation and FTIR Analysis, *Chem. Eng. Res. Des.* 84 (2006) 87–96. <https://doi.org/10.1205/cherd.04036>.
- [62] A. Rivaton, J.L. Gardette, Photodegradation of polyethersulfone and polysulfone, *Polym. Degrad. Stab.* 66 (1999) 385–403. [https://doi.org/10.1016/S0141-3910\(99\)00092-0](https://doi.org/10.1016/S0141-3910(99)00092-0).
- [63] L. Zou, B. Zhu, The synergistic effect of ozonation and photocatalysis on color removal from reused water, *J. Photochem. Photobiol. Chem.* 196 (2008) 24–32. <https://doi.org/10.1016/j.jphotochem.2007.11.008>.
- [64] R. Criegee, Mechanism of Ozonolysis, *Angew. Chem. Int. Ed. Engl.* 14 (1975) 745–752. <https://doi.org/10.1002/anie.197507451>.
- [65] Y. Liu, X. Wang, H. Yang, Y.F. Xie, Quantifying the influence of solute-membrane interactions on adsorption and rejection of pharmaceuticals by NF/RO membranes, *J. Membr. Sci.* 551 (2018) 37–46. <https://doi.org/10.1016/j.memsci.2018.01.035>.
- [66] Y.-L. Lin, Effects of organic, biological and colloidal fouling on the removal of pharmaceuticals and personal care products by nanofiltration and reverse osmosis membranes, *J. Membr. Sci.* 542 (2017) 342–351. <https://doi.org/10.1016/j.memsci.2017.08.023>.
- [67] S.M. Dischinger, J. Rosenblum, R.D. Noble, D.L. Gin, Evaluation of a nanoporous lyotropic liquid crystal polymer membrane for the treatment of hydraulic fracturing produced water via cross-

- flow filtration, *J. Membr. Sci.* 592 (2019) 117313. <https://doi.org/10.1016/j.memsci.2019.117313>.
- [68] Y.-L. Lin, In situ concentration-polarization-enhanced radical graft polymerization of NF270 for mitigating silica fouling and improving pharmaceutical and personal care product rejection, *J. Membr. Sci.* 552 (2018) 387–395. <https://doi.org/10.1016/j.memsci.2018.02.033>.
- [69] N. Park, B. Kwon, I. Kim, J. Cho, Biofouling potential of various NF membranes with respect to bacteria and their soluble microbial products (SMP): Characterizations, flux decline, and transport parameters, *J. Membr. Sci.* 258 (2005) 43–54. <https://doi.org/10.1016/j.memsci.2005.02.025>.
- [70] S. Li, J. Luo, X. Hang, S. Zhao, Y. Wan, Removal of polycyclic aromatic hydrocarbons by nanofiltration membranes: Rejection and fouling mechanisms, *J. Membr. Sci.* 582 (2019) 264–273. <https://doi.org/10.1016/j.memsci.2019.04.008>.
- [71] A.V. Bilyukevich, T.V. Plisko, A.S. Liubimova, V.V. Volkov, V.V. Usosky, Hydrophilization of polysulfone hollow fiber membranes via addition of polyvinylpyrrolidone to the bore fluid, *J. Membr. Sci.* 524 (2017) 537–549. <https://doi.org/10.1016/j.memsci.2016.11.042>.
- [72] Y. Manawi, V. Kochkodan, A.W. Mohammad, M. Ali Atieh, Arabic gum as a novel pore-forming and hydrophilic agent in polysulfone membranes, *J. Membr. Sci.* 529 (2017) 95–104. <https://doi.org/10.1016/j.memsci.2017.02.002>.
- [73] A. Khan, T.A. Sherazi, Y. Khan, S. Li, S.A.R. Naqvi, Z. Cui, Fabrication and characterization of polysulfone/modified nanocarbon black composite antifouling ultrafiltration membranes, *J. Membr. Sci.* 554 (2018) 71–82. <https://doi.org/10.1016/j.memsci.2018.02.063>.
- [74] N. Yang, X. Jia, D. Wang, C. Wei, Y. He, L. Chen, Y. Zhao, Silibinin as a natural antioxidant for modifying polysulfone membranes to suppress hemodialysis-induced oxidative stress, *J. Membr. Sci.* 574 (2019) 86–99. <https://doi.org/10.1016/j.memsci.2018.12.056>.